Crystallographic structure determination of the hairpin ribozyme, a natural catalytic RNA, at ALS beamline 5.0.2

P. B. Rupert and A. R. Ferré-D'Amaré

Division of Basic Sciences, Fred Hutchinson Cancer Research Center,
1100 Fairview Avenue North, Seattle, WA 98109-1024, USA

INTRODUCTION

The hairpin ribozyme is one of four known natural RNAs that catalyze sequence-specific cleavage of RNA. Previous studies suggested that, unlike similar well-characterized ribozymes which rely on bound divalent metal ions to achieve catalysis, the hairpin ribozyme exclusively uses RNA functional groups. The 2.4 Å resolution structure of a hairpin ribozyme-inhibitor complex shows that the active site results from the docking of two irregular helices, stems A and B. There are no tightly-bound metal ions in the catalytic pocket. The nucleotides flanking the scissile bond splay apart, enabling the ribozyme to align the nucleophile and leaving group for the S_N2 reaction. This is the first structure determination of an all-RNA active site assembled to catalyze a phosphodiester cleavage.

BACKGROUND

The hairpin ribozyme is a catalytic RNA derived from the self-cleaving and ligating domain of the negative polarity strand of the satellite RNA of tobacco ringspot virus (sTRSV). *In vivo*, this domain is responsible for generating unit-length circular satellite RNA during the course of its rolling-circle replication (Fig. 1; reviewed in [1]).

Figure 1. Transesterification reaction catalyzed by the hairpin ribozyme. Hypothetical acid and base catalytic groups are indicated. The cleavage reaction generates products with 5'-hydroxyl and 2',3'-cyclic phosphate termini. The hairpin ribozyme does not require any protein or direct coordination to metal ions for full activity, and efficiently cleaves substrate RNAs *in trans*.
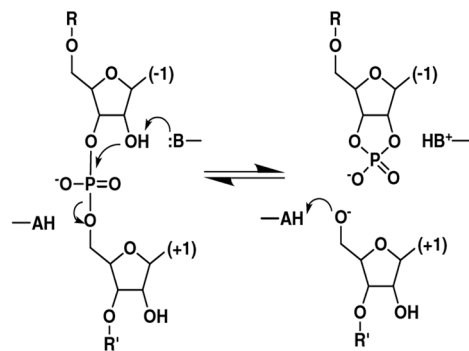
EXPERIMENTAL DESIGN

As a step towards elucidating its catalytic mechanism, and to provide a structural framework for rationalizing the large body of biochemical information previously gathered on this catalytic RNA, we determined the structure of a fully-assembled hairpin ribozyme (Fig. 2). We crystallized a four-helix junction form of the RNA, complexed with a substrate strand in which the nucleophilic 2'-OH group was replaced with a methoxy function. Crystals were grown in the presence of 20 mM Ca^{2+}, enough to saturate the structural metal ion-binding sites. To facilitate the growth of well-ordered crystals[2], the cognate site for the RNA-binding protein U1A was grafted onto the structurally and functionally dispensable[1] distal end of stem B (Fig. 2). The

modification and binding of U1A had no effect on ribozyme activity. The engineered RNA was cocrystallized with the basic protein.

Figure 2. Overall structure of the hairpin ribozyme. **a**. Secondary structure of the hairpin ribozyme used for crystallization. Gray regions represent functionally dispensable sequences and include the cognate sequence of the U1A binding site. The four-helix junction is cyan, stem B is green, and stem A is red and orange. In the red substrate strand, the two nucleotides adjacent to the scissile bond are light blue. The arrow indicates the cleavage site. **b**. Three-dimensional structure of the hairpin ribozyme. The RNA backbone is depicted schematically as ribbons; the nucleotide bases, as sticks (color as in part a). The four selenium atoms in the U1A protein are shown as magenta spheres. Three RNA-bound calcium ions are depicted as blue spheres.
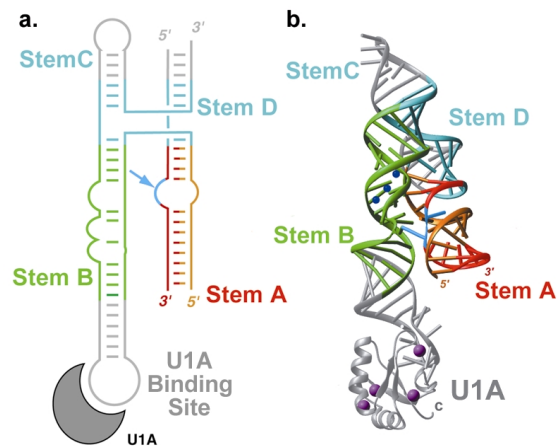
STUDIES CONDUCTED AT THE ADVANCED LIGHT SOURCE

We obtained crystals of the hairpin ribozyme with the symmetry of space group *C2,* and unit cell dimensions $a = 256.3$ Å, $b = 44.1$ Å, $c = 102.4$ Å, and $\beta = 109°$. Crystals were flash-frozen after stabilization in a synthetic mother liquor containing 30 % MPD. Experimental phases were obtained to 2.9 Å resolution by the MAD method using a crystal containing a selenomethionine version of the U1A protein. The MAD diffraction data were collected at three different wavelengths corresponding to the inflection point, peak, and a high energy remote for selenium as determined from a fluorescence scan of the actual crystal. Given the low symmetry of the crystals, in order to obtain complete anomalous data sets, 360° of data were collected at both the peak, and remote wavelengths. In addition, 180° of data were collected at the inflection point wavelength. The three X-ray energies remained very stable over the eight hours of data collection. Despite the small number of selenium atoms (four per 47 kDa macromolecular complex), there was sufficient signal to locate the selenium sites in Patterson maps (Fig. 3). All the major peaks on the Harker section could be accounted for as either self or cross peaks.

Figure 3. Harker sections calculated from hairpin ribozyme diffraction data. The top section shows the averaged experimental Patterson map calculated using both the anomalous difference at the peak wavelength of the selenium K edge and the dispersive differences between inflection wavelength and the high energy remote wavelength. The lower section shows predicted peaks based on the correctly identified selenium sites.
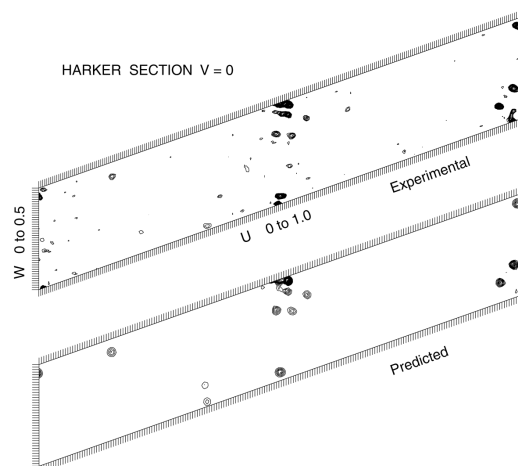
Because the crystals contained 65% solvent, 'solvent flattening' considerably improved the experimental electron density. The electron density allowed us to unambiguously build in all of the RNA residues and most of the protein residues (Fig 4). The high resolution 2.4 Å data set

was collected at beamline 5.0.2. using the X-ray energy of maximum flux ($\lambda = 1.1\text{Å}$). We first measured the weak high-resolution reflections with long exposures, and then the strongly-diffracting low-resolution reflections with short exposures. This data set was 95.6% complete between 100 – 2.4 Å (73.9% between 2.5 – 2.4 Å), with an R_{merge} of 6.7 %(26.1%). Even though the diffraction data are weak at high resolution (Wilson $B = 66 \text{ Å}^2$), the signal-to-noise ($<I>/<\sigma(I)>$) is 2.1 in the highest resolution data shell (2.5 –2.4 Å). The structure has been refined to an R-factor of 24.7 % (R-free = 28.9 %).

Figure 4. Representative 'solvent flattened' experimental MAD electron density around the cleavage site, superimposed on the refined model. The extrusion of G+1 from stem A results in an in-line arrangement of the nucleophile (2'-OH of A-1, right arrow) and leaving group (5'-OH of G+1, left arrow) relative to the phosphorous atom at the reaction site. The electron density is contoured at one standard deviation above mean peak height.
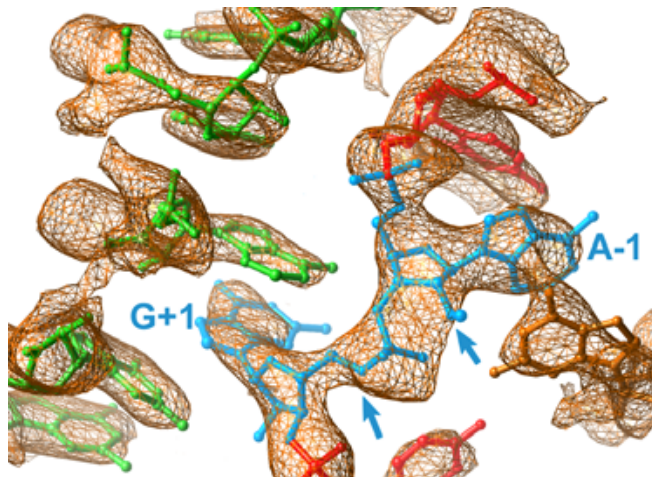
In the crystal structure, the four helical stems that comprise the hairpin ribozyme radiate from a perfectly base-paired four-way junction (Fig. 2b). These helices form two coaxial stacks: stem D stacks on A, and stem C on B. The two stacks cross at a ~60° angle, and are connected by a pair of anti-parallel crossovers (Fig. 2). The conformation of the junction allows docking of the minor grooves of the central portions of stems A and B to form the active site of the ribozyme. The crystal structure shows that the active site is entirely comprised of RNA (Fig. 4). This implies that the RNA itself provides functional groups that accomplish acid-base catalysis.

ACKNOWLEDGMENTS

REFERENCES

1. Fedor MJ. Structure and function of the hairpin ribozyme. *J Mol Biol* **297**, 269-91 (2000).
2. Ferré-D'Amaré AR, Z. K., Doudna JA. Crystal structure of a hepatitis delta virus ribozyme. *Nature* **395**, 567-74 (1998).

Principal investigator: Adrian R. Ferré-D'Amaré, Fred Hutchinson Cancer Research Center, 1100 Fairview Avenue North, Seattle, WA 98109-1024. Email: aferre@fhcrc.org. Telephone: 206-667-3622.